Parametric instability of shaft with discs

A M Abdul Wahab, Z A Rasid*, A Abu and N F Mohd Noor Rudin

Malaysia-Japan International Institute of Technology, Kuala Lumpur, Malaysia.

*arzainudin.kl@utm.my

Abstract. The occurrence of resonance is a major criterion to be considered in the design of shaft. While force resonance occurs merely when the natural frequency of the rotor system equals speed of the shaft, parametric resonance or parametric instability can occur at excitation speed that is integral or sub-multiple of the frequency of the rotor. This makes the study on parametric resonance crucial. Parametric instability of a shaft system consisting of a shaft and disks has been investigated in this study. The finite element formulation of the Mathieu-Hill equation that represents the parametric instability problem of the shaft is developed based on Timoshenko's beam theory and Nelson's finite element method (FEM) model that considers the effect of torsional motion on such problem. The Bolotin's method is used to determine the regions of instability and the Strut-Ince diagram. The validation works show that the results of this study are in close agreement to past results. It is found that a larger radius of disk will cause the shaft to become more unstable compared to smaller radius although both weights are similar. Furthermore, the effect of torsional motion on the parametric instability of the shaft is significant at higher rotating speed.

1. Introduction

There are two types of resonance: force resonance and parametric resonance. In rotor-dynamic field of study, the force resonance has been widely researched [1-4]. It can result in catastrophic failure of the rotor system if the external excitation such as the speed of the shaft equals to the natural frequency of the rotor system. Parametric resonance or parametric instability of a rotor system, on the other hand, occurs due to external excitation that modifies the stiffness, inertia or other parameters of the rotor system with time. In comparison to force resonance, parametric instability can occur more often at the excitation speeds that are integral or sub-multiple of the frequency of the rotor. This highlights the importance of the study on the parametric instability of the rotor system. Furthermore, the parametric instability of the rotor system can lead to its fatigue failure [5]. Many research have been devoted on improving parametric instability of rotor systems subjected to periodic changes of inertia or stiffness that could be due to the anisotropic bearing support [6], asymmetry of disk and shaft [7], periodic axial compressive load [8] and the transverse crack propagation [9].

Studies on dynamic instability analysis of a rotating beam/shaft subjected to periodic axial forces have been conducted using the discrete singular convolution method [10-11]. While considering the external viscous damping and internal material damping, it has been shown that the instability region increases with the increase of spinning speed for shaft with damping, and the results correlated well with those obtained using the Floquet's method. In addition, the instability region can also be modified by shear deformation, rotatory inertia, distributed axial loads, elastic soil and damping [12]. In term of damping, it has been suggested that internal damping of the Kelvin-Voigt has stabilizing effect on the

primary parametric resonance dynamic instability of Timoshenko beam under the periodic axial loads [13]. However, it depends on the size of the damped segment and its location. The system is stable if the damped segment is located near the fixed end where it enlarged from the fixed end. On the other hand, static load component has destabilizing effect to the shaft system as it is increased. Recently, a study has shown that the location of disk has significant effect on dynamic instability of a shaft system [14]. Using the transfer matrix method, the critical axial force is found to decrease rapidly at first, then remains almost constant, and finally decreases linearly as the disk is located closer to the support at the right end when shear deformation is not considered.

Nonetheless, the above studies do not focus on shafts that may rotate at very high speed. Machines that operate at high shaft speed are well sought nowadays since high overall efficiency of the rotating equipment can be achieved when the speed of the rotating equipment lies in between 10000 RPM and 100000 RPM [15]. Furthermore, while focusing on the effects such as translational and rotary inertia, gyroscopic moments, bending and shear deformation, and damping, an important effect of axial torque of the shaft has been neglected. Though the effect of axial torque has been applied by Nelson (1980) [16] and Rao (2011) [17], their studies are limited to the whirling frequency and critical speed of the shaft. In this study, apart from focusing on the effect of attaching discs to the shaft, the parametric instability of high speed rotor system subjected to periodic axial load is investigated while considering the effect of the axial torque. The shaft speed is up to 40000 RPM. The disc parameters under study here are the disk location with respect to shaft, disk mass and the number of disc. The finite element method (FEM) form of the Mathieu-Hill equation is developed considering the translational and rotary inertias, gyroscopic moments, bending and shear deformations, and the axial torque. The results are validated and compared with those from the formulation that does not consider the axial torque effect.

2. Material and Methods

The rotor system investigated in this study consists of a shaft, one or more discs and two bearings, represented by the supports as shown in Figure 1. L and *l* are the length of the shaft and the distance of the disk from the left bearing, respectively, while d and t are the diameter of the shaft and thickness of the disk, respectively. Table 1 shows the material properties and the dimensions of components of the rotor system being investigated.

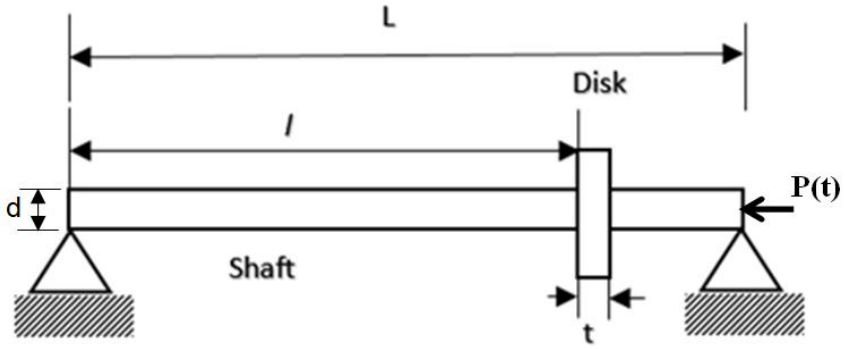

Figure 1: The rotor system being investigated

This study employs FEM to estimate the whirling natural frequency and the parametric instability region of the rotating shaft system. The developed FE formulation is based on Ref. [15], where the Timoshenko beam theory and the Nelson's FEM approach that considers the torsional effect are used. The effect of torsional motion is added to the formulation as the degree of freedom such that its effect on resonance can be determined. In this study, beam model having elements with 5 degrees of freedom per node including the axial twist of the shaft is called the 5DOF model. The results will be compared to those of the beam model having element with 4 degrees of freedom per node that is 4DOF model. Figure 2 shows the degrees of freedom of the shaft element used in this study. The model involves two

translation components and three rotary inertia components that are denoted by v, ω, θ_x, θ_y and θ_z, respectively. The translation components are due to bending, transverse shear deformation and also torsional motions. Meanwhile, the rotary inertia components are due to bending and torsional motions.

Table 1: Dimensions and material properties of the shaft system in the study on the effect of the location of disc (Study 1), the mass of the disc (Study 2) and the number of discs attached (Study 3)

Shaft	
Young's modulus, E	207 GPa
Modulus of rigidity, G	79.6 GPa
Poisson's ratio, v	0.303
Density, ρ	7833 kg/m^3
Radius, r	round tube with r_{inner} = 0 m, r_{outer} =0.0508 m
Length, L	1.27 m
Shear factor, κ	0.9
Bearing	
Direct stiffness coefficient, K_{by}, K_{bz}	7x10^{7}N/m
Direct damping coefficient, C_{by},C_{bz}	0
Disk in Study 1	
Young Modulus, *E*	207 GPa
Density, ρ	7833 kg/m^3
Thickness, t	0.03 m
Diameter, d	0.3 m
Disk in Study 2	
Young Modulus, *E*	207 GPa
Density, ρ	7833 kg/m^3
Diameter, d_1 and d_2	0.3 m
Thickness, nominal weight, t_1	0.03 m
Thickness, heavy weight, t_2	0.07 m
Diameter, d_3	0.16 m
Thickness, nominal weight, t_3	0.1055 m
Disk in Study 3	
Young Modulus, *E*	207 GPa
Density, ρ	7833 kg/m^3
Diameter, d_1, d_2	0.4 m
Thickness, t_1, t_2	0.005 m
Diameter, d_3	0.4 m
Thickness, t_3	0.006 m

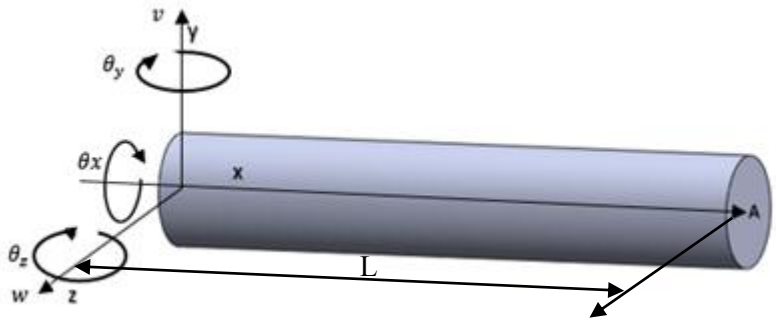

Figure 2: The displacement and rotational degree of freedom components of a shaft element

In Figure 1, the rotating shaft is loaded with a pulsating axial force, $P(t)$ (given by Equation 1) that acts along the un-deformed axis of the shaft. Component ϕ denotes the frequency axial excitation of the dynamic force component. P_s and P_t are the static and time dependent components of the force, respectively.

$$P(t) = P_s + P_t \cos \phi t \tag{1}$$

The total potential energy stored in the beam element that is due to bending and torsional motions can be expressed as in Equation 2, where E is the Young's modulus of the shaft, G is the shear modulus of the shaft, I_p is the total second moment of inertia, J is the polar moment of inertia, A is cross-sectional area of the shaft, k is the shear correction factor, P is the axial force and θ_x, θ_y and θ_z are the rotary displacement in x-, y- and z-axis, respectively.

$$U = \frac{1}{2}\int_{-a}^{+a} EI_p(\acute{\theta}_z^2 + \acute{\theta}_y^2)\ dx + \frac{1}{2}\int_{-a}^{+a} \kappa GA(\acute{v} - \theta_z)^2 + \kappa GA\left(\acute{w} + \theta_y\right)^2\ dx + \frac{1}{2}\int_{-a}^{+a} GJ\acute{\theta}_x^2\, dx - \frac{1}{2}\int_{-a}^{+a} P[(\acute{v})^2 + (\acute{w})^2]dx \tag{2}$$

$$I_p = I_z + I_y = \int z^2\, dA + \int y^2\, dA \tag{3}$$

$$J = \int_{-a}^{+a} \left(\frac{\partial \psi}{\partial y} - z\right)^2 + \left(\frac{\partial \psi}{\partial y} + y\right)^2\ dA \tag{4}$$

$$\acute{\theta} = \frac{\partial \theta}{\partial x} \tag{5}$$

$$\acute{v} = \frac{\partial v}{\partial x} \tag{6}$$

On the other hand, kinetic energy of the rotating shaft is given by Equation 7, where the first, second, third and fourth terms correspond to translation energy term, rotary inertia term, gyroscopic element and torsional element terms, and ρ is the density of the shaft.

$$T = \frac{1}{2}\int_{-a}^{+a} \rho A\left(\left(\frac{\partial v}{\partial t}\right)^2 + \left(\frac{\partial w}{\partial t}\right)^2\right) dx + \frac{1}{2}\int_{-a}^{+a} \rho I_y\left(\frac{\partial \theta_y}{\partial t}\right)^2 + \rho I_z\left(\frac{\partial \theta_z}{\partial t}\right)^2\ dx + \frac{1}{2}\int_{-a}^{+a} \rho I_x\left(\frac{\partial \theta_x}{\partial t}\right)^2\ dx \tag{7}$$

The shaft under study is discretized into several elements and each element consists of two nodes. Following the standard FEM procedure and using Lagrange's formula, the standard FEM governing equation is given by Equation 8, where $[M]$, $[G]$, $[K]$ and $[K_g]$ are the elemental mass, gyroscopic, stiffness and geometric stiffness matrices, respectively, Ω is the spin speed, $P(t)$ is the periodic axial force and $\{q\}$ is the nodal displacement vector.

$$[M]\{\ddot{q}\} + \Omega[G]\{\dot{q}\} + ([K] - P(t)[K_g])\{q\} = 0 \tag{8}$$

The periodic axial force can be written as $P(t) = \alpha P^* + \beta P^* \cos \phi T$ where α and β are the static and dynamic load factors, respectively. Then, the Mathieu-Hill type of equation is given as Equation 9.

$$[M]\{\ddot{q}\} + \Omega[G]\{\dot{q}\} + ([K] - [K_g](\alpha P^* + \beta P^* \cos \phi T(t))\{q\} = 0 \tag{9}$$

The Bolotin's method converts Equation 9 into Equation 10 that represents the parametric instability problem to be solved in this study. Equation 10 gives an infinite eigenvalue problem as indicated by Equation 11, or in full form as shown by Equation 12.

$$(\phi^2[M_E] + \phi[G_E] + [K_E])q = 0 \tag{10}$$

$$|(\phi^2[M_E] + \phi[G_E] + [K_E])| = 0 \tag{11}$$

$$\left\| \begin{bmatrix} [K] + \left(\alpha - \frac{\beta}{2}\right)[K_g] & 0 \\ 0 & [K] + \left(\alpha + \frac{\beta}{2}\right)[K_g] \end{bmatrix} + \phi \begin{bmatrix} 0 & -\frac{1}{2}\Omega[G] \\ \frac{1}{2}\Omega[G] & 0 \end{bmatrix} + \phi^2 \begin{bmatrix} -\frac{1}{4}[M] & 0 \\ 0 & -\frac{1}{4}[M] \end{bmatrix} \right\| = 0 \tag{12}$$

3. Results and Discussion

Dynamic instability analysis is conducted on the static and rotating simply supported shafts, subjected to axial compressive load. The results are then compared to the work of Chen and Ku (1990) [18] that applied Timoshenko beam element, which requires four degrees of freedom per node. Figure 3 shows the plots of dynamic load factor, β against the frequency ratio that represents the parametric instability regions for the shafts, where regions in between the V-shape lines represent the instability region (**US**). For other regions (**S**), the system goes toward stable equilibrium position as disturbance occurs. Figure 3 also shows that the instability regions of current works are in good agreement with Ref. [18].

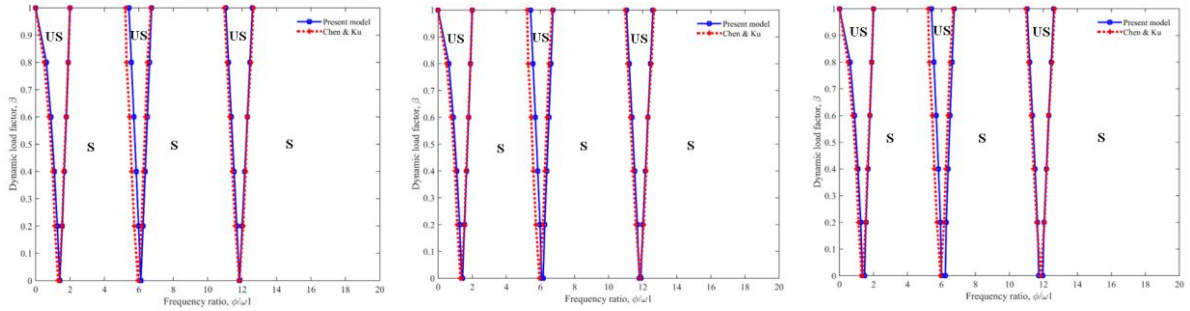

(a) (b) (c)

Figure 3: Validation of the dynamic instability charts for simply supported shaft at: (a) 0 RPM, (b) 8000 RPM (c) 20000 RPM

In reference to Table 1, three cases are compared in this study: Case 1 - shaft without any disk (no disk), Case 2 – shaft with a disk located at the middle of the shaft (disk @ 50%) and Case 3 – shaft with a disk positioned near to the end of the shaft (disk @ 75%). Disk with the same properties is used throughout the analysis. Case 1 (no disk) is used as the benchmark for any difference that might occur in the dynamic behaviour of the shaft as the disk is added. Rigid bearings are used in this study. Figure 4 to Figure 6 show the plots of instability regions of the shaft at 0 RPM, 9000 RPM and 40000 RPM, respectively, for the three cases of disk location based on 4DOF and 5DOF models. In all cases, as the position of the disc is moved to the right, the instability charts can be seen to be moved to the left. This shows that having the disk location near to the end of shaft results in more unstable shaft as compared to having the disk placed at the center of shaft, which is in line with the work in Ref. [14]. Comparing the plots corresponding to 4DOF and 5DOF models, the effect of torsion considered in 5DOF model is significant at high speed. At high speed, the plots have no centre of instability whereas the instability region for 5DOF model can be seen to be wider, which indicates that the torsional effect has increased the instability of the shaft. The difference in frequency ratio between that of 4DOF model and 5DOF model reaches 60% at the spin speed of 40000 RPM.

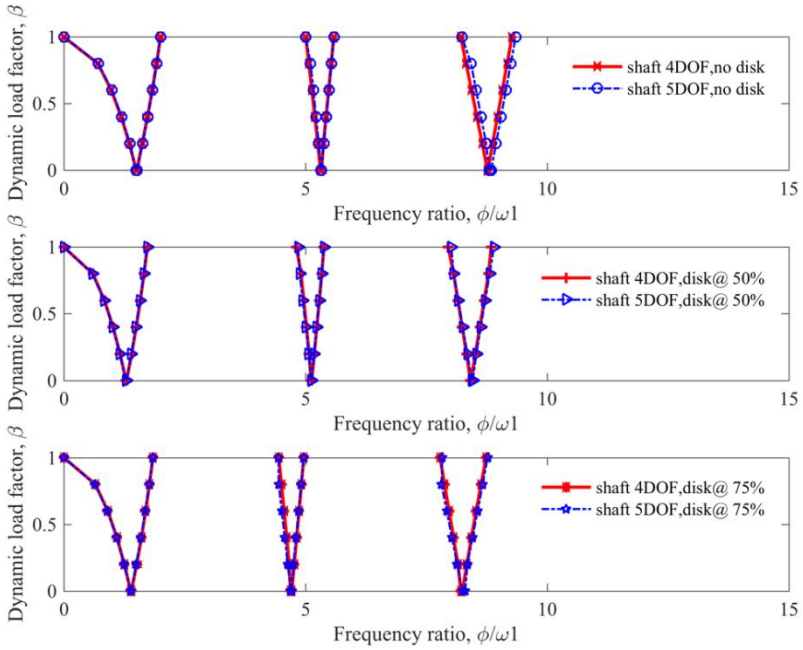

Figure 4: Effect of location of disk on dynamic instability of the shaft rotating at 0 RPM

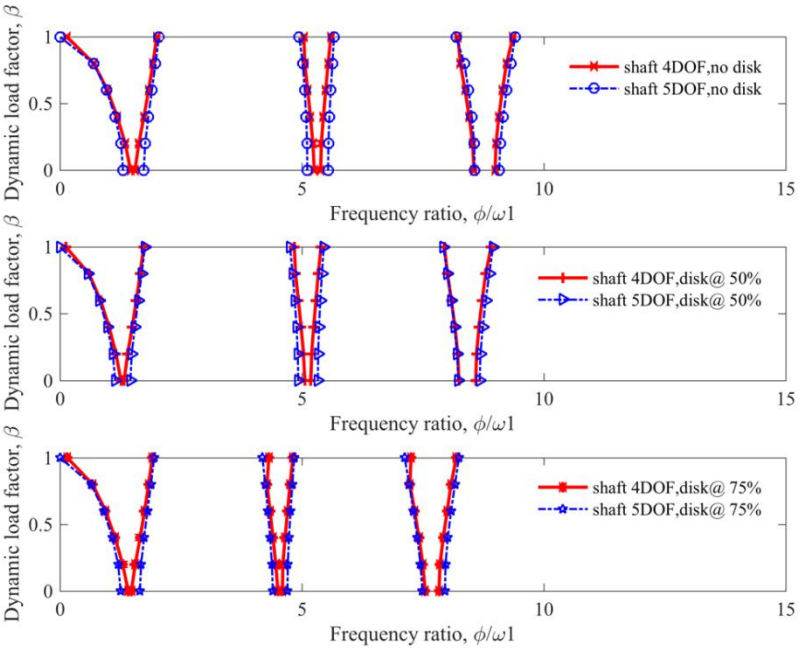

Figure 5: Effect of location of disk on dynamic instability of the shaft rotating at 9000 RPM

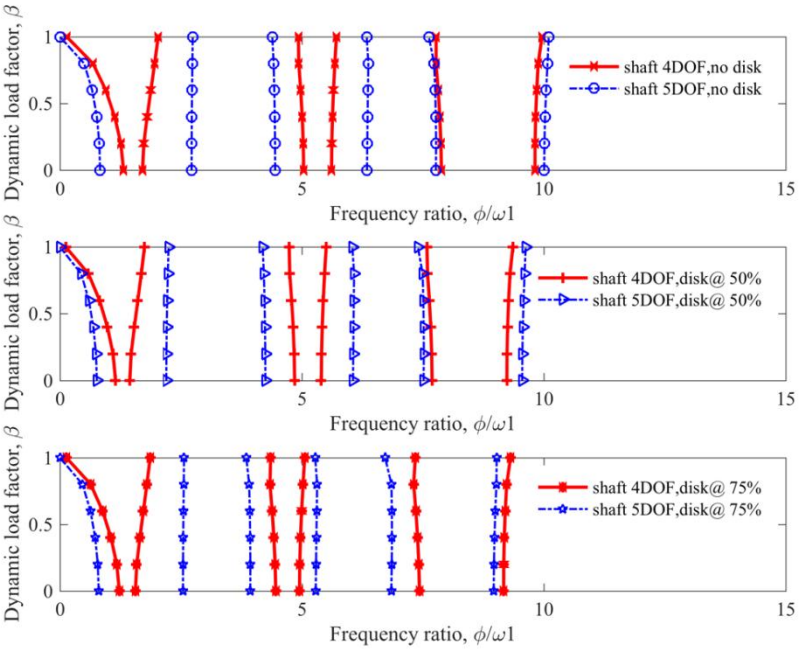

Figure 6: Effect of location of disk on dynamic instability of the shaft rotating at 40000 RPM

Moreover, the effect of disk mass on the dynamic behaviour of shaft is also studied. In reference to Table 1, for Study 2, a rotor with rigid bearings and centred single disk is used. The comparison is between nominal disk, heavy disk and nominal thick disk to be attached to the shaft. The nominal disk and the nominal thick disk differ in their radius and thickness but their masses are the same. Figure 7 to Figure 9 depict the plots of dynamic load factor, β against frequency ratio that show the instability regions of the shaft at 0 RPM, 9000 RPM and 40000 RPM, respectively, modelled using 4DOF and 5DOF models. The advantage of using 5DOF model can be seen at higher rotational shaft speed where the dynamic instability chart is wider due to torsional degree of freedom effect that is considered in 5DOF model. The wider instability chart of the 5DOF model as compared to that of the 4DOF model can be seen at 9000 RPM and even much clearer at 40000 RPM. Figure 7 shows that the parametric instability regions of shafts consisting of the three disk types are quite similar at static condition. In Figure 9, at rotational shaft speed of 40000 RPM, parametric instability corresponding to the nominal disk is more stable compared to that of the heavy disk according to the 5DOF model. However, the instability region for nominal disk can be seen to slightly shift towards the higher frequency level as compared to that of the nominal thick disk. This makes the shaft becomes more stable in the case of disk with smaller radius. The width of disk centre orbit of the shaft system is proportional to the radius of the disk while at the same time, the instability condition depends on the width of disk centre [19]. Therefore, for disks with equal weight, as the axial force fluctuates, the one with larger radius is more unstable compared to that of smaller radius.

In the meantime, the comparison made in Study 3 from Table 1 is on the dynamic behaviours of shafts having one, two and three disks. In all cases, rigid bearings are used to support the shaft at both its ends. Figure 10 to Figure 12 show the plots of dynamic load factor, β against the frequency ratio corresponding to shafts having one, two and three number of disks at a speed of 0 RPM, 9000 RPM and 40000 RPM, respectively, where 4DOF and 5DOF models are applied. In all cases, the increase in the number of disk will shift the instability region inward, showing that the shaft becomes unstable as the number of disk increases although the width of the instability chart remains equal. This condition is expected since natural frequency is inversely proportional with mass. The effect of torsional degree of freedom considered in the 5DOF can be seen in the widening of the parametric instability chart as the

speed is increased. In general, the width of instability region increases as rotating speed increases, thus making the system more unstable at higher speed.

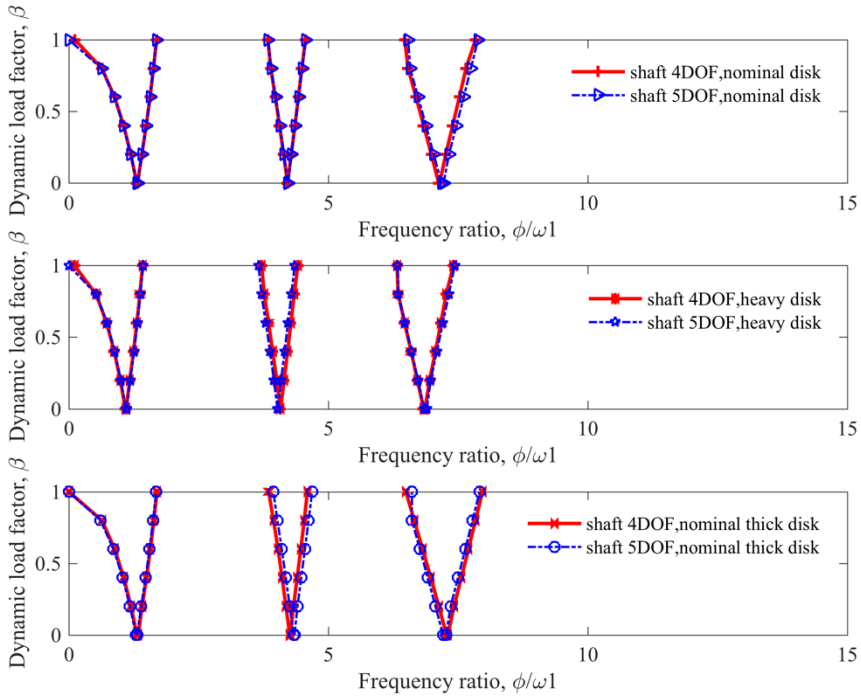

Figure 7: Effect of disk mass on parametric instability of shaft at 0 RPM

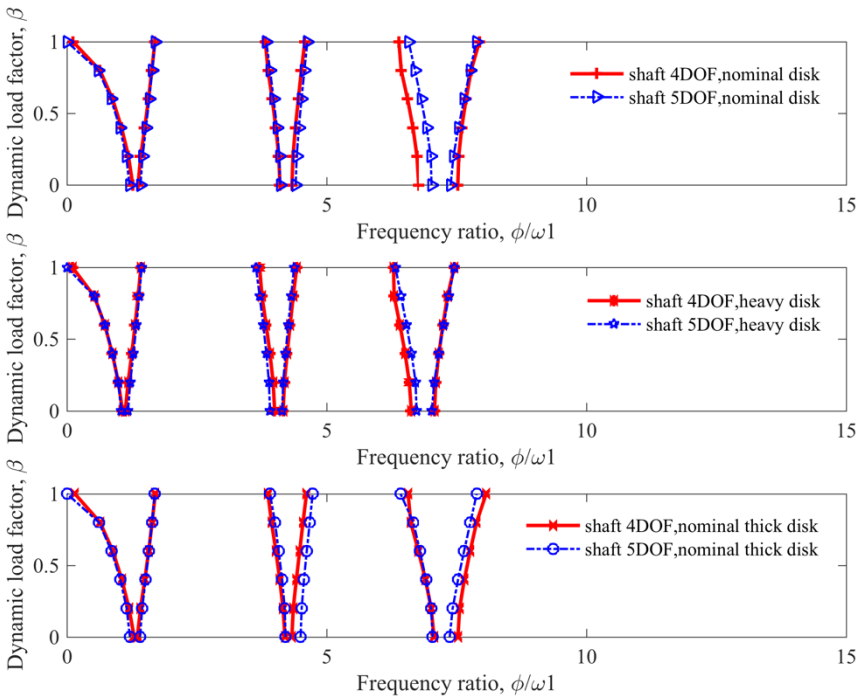

Figure 8: Effect of disk mass on parametric instability of shaft at 9000 RPM

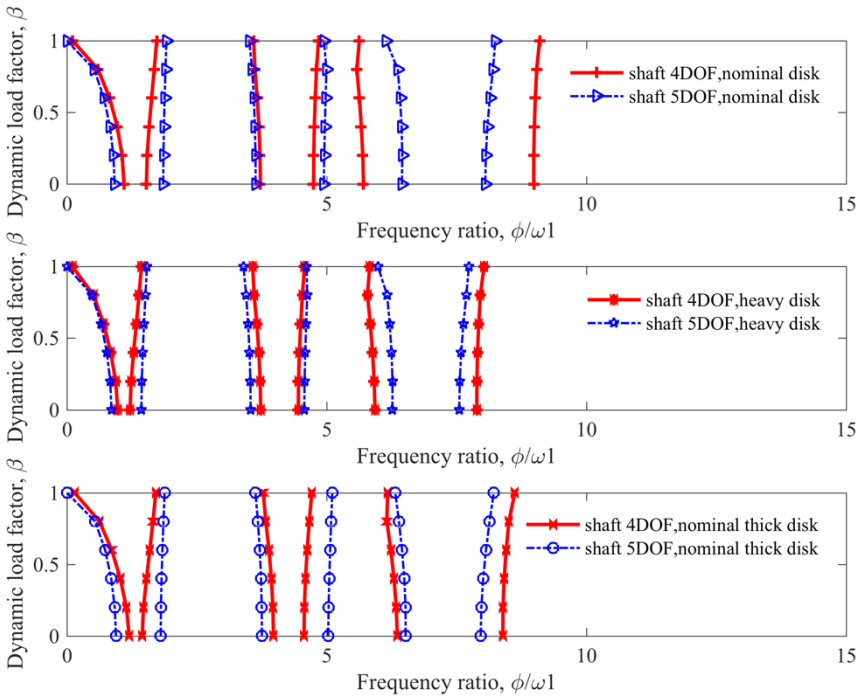

Figure 9: Effect of disk mass on parametric instability of shaft at 40000 RPM

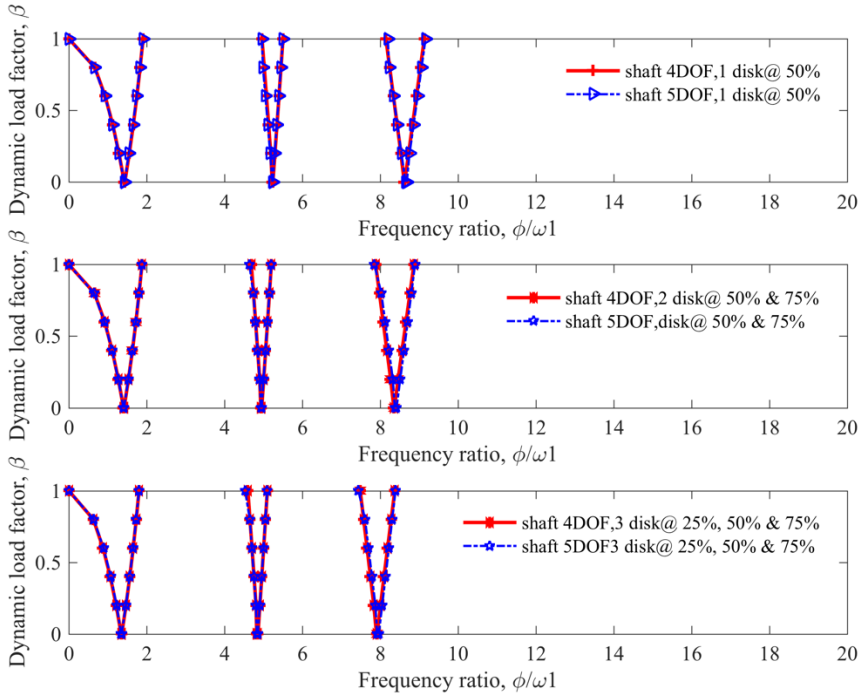

Figure 10: Effect of number of disk on parametric instability of shaft at 0 RPM

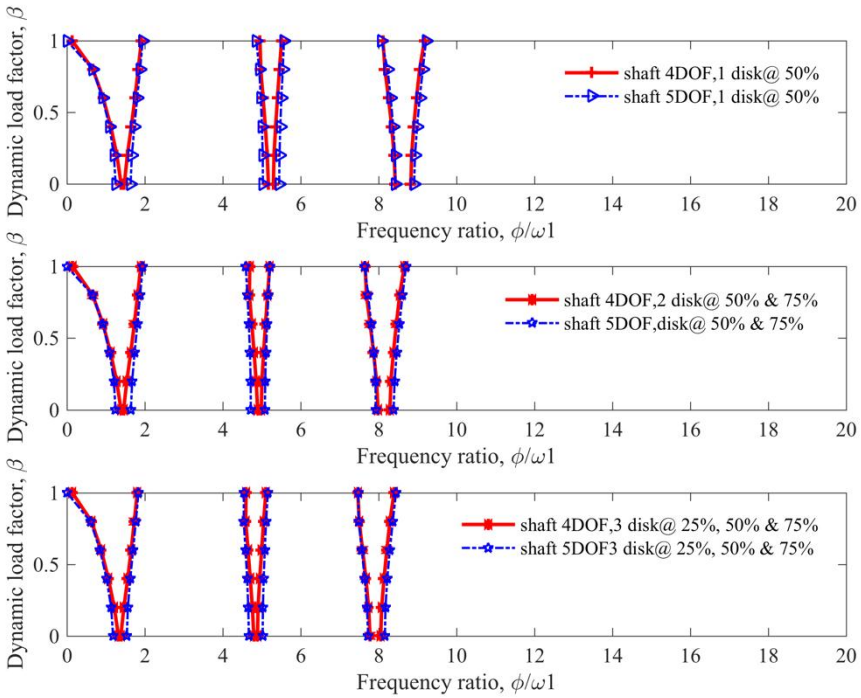

Figure 11: Effect of number of disk on parametric instability of shaft at 9000 RPM

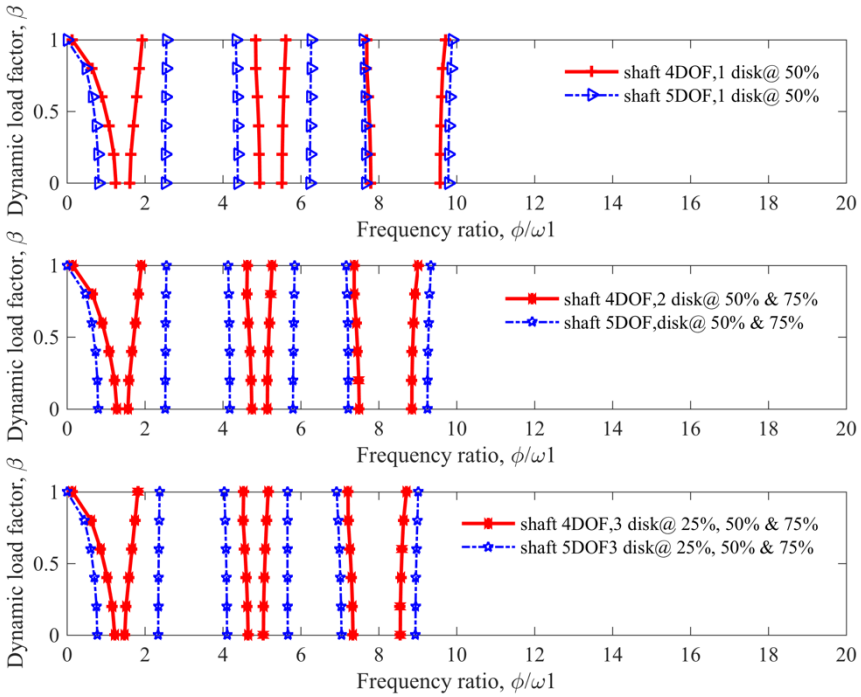

Figure 12: Effect of number of disk on parametric instability of shaft at 40000 RPM

4. Conclusion

A study has been conducted on the effect of attaching disks on the parametric instability of high speed shaft while considering the torsional effect of the shaft. Two FEM formulations (i.e. 4DOF and 5DOF models) are developed for parametric instability study of shaft, where the latter model considers the torsional effect of the shaft. In general, the width of instability region of a shaft increases as rotating speed increases, thus the system becomes more unstable at higher speed. Furthermore, the instability charts corresponding to the 5DOF model show wider instability region as compared to those of 4DOF model at high speed. This shows that the torsional effect has caused the rotor system to become more unstable at high speed and the difference in the width of the instability chart can reach as high as 60% at the spin speed of 40000 RPM for the case of the effect of disk location in study 1. As such, it can be concluded that, for the shaft-disk system, the effect of torsional motion of the shaft on the parametric instability of the shaft is significant at higher rotating speed. Moreover, a rotor system becomes more unstable at lower frequency as the number of disk increases and, for static shafts with disks that differ in weight and radius, their parametric instability regions are quite similar. Last but not least, attaching disk with larger radius will cause the shaft to become more unstable.

Acknowledgement

The authors acknowledge the support in this study from Malaysia-Japan Institute of Technology and Universiti Teknologi Malaysia through the provision of the GUP Tier 2 Grant – PY/2017/00468.

References

[1] Gayen D, Chakraborty D and Tiwari R 2017 *European Journal of Mechanics A/Solids* **61** 47-58
[2] Bai B, Zhang L, Guo T and Liu C 2012 *Procedia Engineering* **31** 654–8
[3] Hu Z, Tang J, Zhong J, Chen S and Yan H 2016 *Mechanical Systems and Signal Processing* **76-77** 294–318
[4] Montagnier O and Hochard C 2014 *Journal of Sound and Vibration* **333** 470–84
[5] Bolotin V V 1965 *Am. J. Physics* **33** 752
[6] Wang S, Wang Y, Zi Y and He Z 2015 *Journal of Sound and Vibration* **359** 116-35
[7] Mailybaev A A and Spelsberg-Korspeter G 2015 *Journal of Sound and Vibration* **336** 227-39
[8] Chen W R and Chen C S 2014 *International Journal of Structural Stability and Dynamics* **14** 1-24
[9] Han Q and Chu F 2012 *Communication in Nonlinear Science Numerical Simulation* **17** 5189-200
[10] Li W, Song Z and Chai Y 2015 *Journal of Engineering Mechanics* **141** 04015033
[11] Song Z, Chen Z, Li W and Chai Y 2017 *Meccanica* **52** 1159-73
[12] Dakel M, Baguet S and Dufour R 2014 *Journal of Sound and Vibration* **333** 2774-99
[13] Chen W R and Chen C S 2014 *International Journal of Structural Stability and Dynamics* **14** 1450014
[14] Yim K B and Yim J T 2013 *J. Mech. Sci. Technology* **27** 359–66
[15] Boglietti A, Gerada C and Cavagnino A 2014 *IEEE Trans. Ind. Electron* **61** 2943-5
[16] Nelson H D 1980 *Journal of Mechanical Design* **102** 793-803
[17] Rao J S 2011 *Finite Element Methods for Rotor Dynamics* in *History of Rotating Machinery Dynamics* Springer Netherlands
[18] Chen L W and Ku D M 1990 *J. Sound Vibration* **143** 143–51
[19] Pei Y C, Lu H and Chatwin C 2010 *Proc. Inst. Mech. Eng. Part K J. Multi-Body Dynamics* **224** 211–9